Netherlands Journal of Geosciences — Geologie en Mijnbouw | 89 – 3/4 | 173 - 186 | 2010

The timing of aeolian events near archaeological settlements around Heidebos (Moervaart area, N Belgium)

C. Derese[1,*], D.A.G. Vandenberghe[1], A. Zwertvaegher[2], M. Court-Picon[3], P. Crombé[4], J. Verniers[3] & P. Van den haute[1]

1 Laboratory of Mineralogy and Petrology (Luminescence Research Group), Department of Geology and Soil Science, Ghent University, Krijgslaan 281 (S8), B-9000 Gent, Belgium.
2 Laboratory of Soil Science, Department of Geology and Soil Science, Ghent University, Krijgslaan 281 (S8), B-9000 Gent, Belgium.
3 Laboratory of Palaeontology, Department of Geology and Soil Science, Ghent University, Krijgslaan 281 (S8), B-9000 Gent, Belgium.
4 Prehistory and Protohistory Research Group, Department of Archaeology, Ghent University, Sint-Pietersnieuwstraat 35 (Ufo), B-9000 Gent, Belgium.
* Corresponding author. Email: cilia.derese@ugent.be.

Manuscript received: July 2010, accepted: December 2010

Abstract

At the locality of Heidebos (Moervaart area, N Flanders, Belgium), a sedimentary core was taken in the Maldegem-Stekene coversand ridge and dated using optically stimulated luminescence (OSL). The study aimed at contributing to an improved understanding of the evolution of the physical landscape around archaeological settlements in this area. The core comprised a 7 m thick series of laminated and massive aeolian sands, in which several organic layers were intercalated. From this sequence, 11 samples were collected for quartz-based SAR-OSL dating; an internally consistent dataset was obtained. The ages of the lowermost 1 m of the sedimentary sequence (15.5±1.1 ka and 17.3±1.3 ka) imply that these sediments may represent the time-equivalent deposit of a deflation phase that occurred during the Late Pleniglacial and led to the formation of a widespread desert pavement, regionally known as the Beuningen Gravel Bed. However, a significant part of the sediments (at least 4 m) was deposited later, i.e. during the Allerød and/or the Late Dryas. As such, the results allow establishing the genesis of the coversand ridge at the Heidebos locality on the basis of direct age information. The relatively high sedimentation rate and the absence of extensive soil formation in the record reflect periods of pronounced aeolian activity and landscape instability during the Late Glacial, which provides part of the environmental framework for human occupation in the area.

Keywords: Late Glacial; Maldegem-Stekene coversand ridge; Moervaart depression; NW European coversand belt; Optically stimulated luminescence dating; Quartz

Introduction

In NW Europe, the Weichselian-Holocene transition period has been the focus of a multitude of studies investigating the interaction between past human societies and their natural environment (e.g. Bos & Janssen, 1996; De Bie & Vermeersch, 1998; Street, 1998). This period, the so-called Late Glacial, was marked by pronounced climatic and environmental changes, which had a major influence on the human migration patterns and the regional distribution of human settlements. The time boundaries of the Late Glacial, as well as of all other chronostratigraphical and archaeological periods mentioned below, are summarised in Fig. 1. An overview of the human occupation in the NW European lowlands was provided by De Bie & Vermeersch (1998) and Deeben & Rensink (2005). According to these authors, the area remained uninhabited until after the Last Glacial Maximum (~21 ka cal BP). Palaeolithic hunter-gatherer societies presumably reached the NW European lowlands (Belgium and the Netherlands) around 13 ka ^{14}C BP (~15.5 ka cal BP), and settled in the Belgian loess belt and

https://doi.org/10.1017/S0016774600000688 Published online by Cambridge University Press

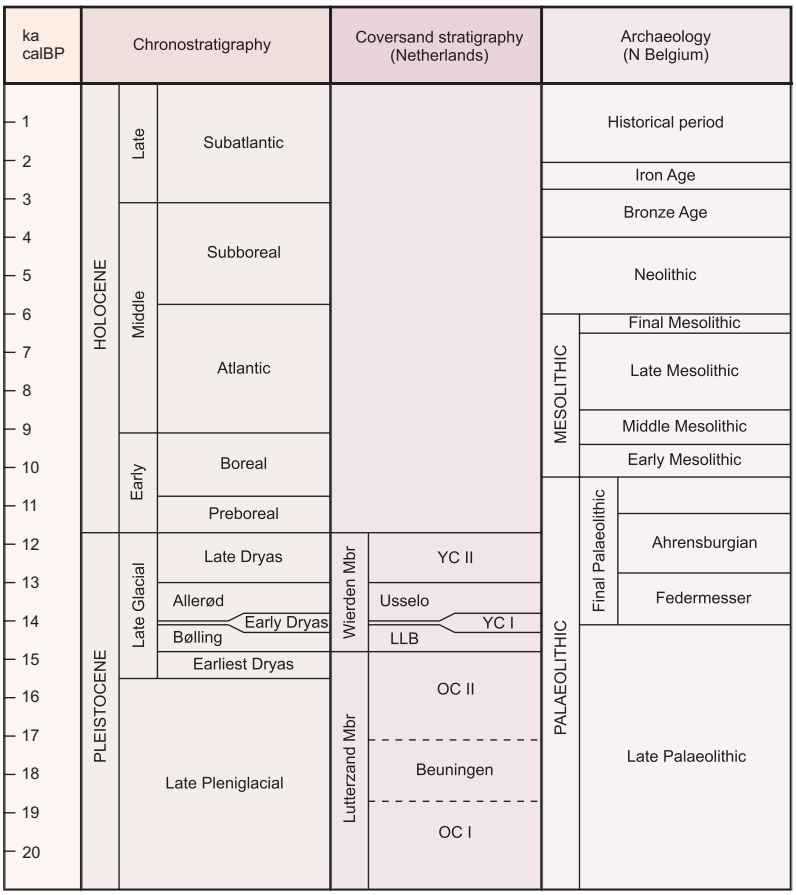

Fig. 1. Table summarising the subdivision of the last ~20 ka in terms of chronostratigraphy, coversand stratigraphy and archaeology. The chronostratigraphical subdivision of the Late Pleistocene is based on the ^{14}C dated time boundaries of the pollen zones (revised by Hoek, 2001), that of the Holocene is based on Terberger et al. (2009). Calibration of the radiocarbon ages was carried out using OxCal 4.1 (Bronk Ramsey, 2009) and the IntCal09 calibration curve (Reimer et al., 2009), and they are expressed as the 68.2% probability interval (unless stated differently) before AD 2000 ('BP') to allow comparison with the OSL ages. The stratigraphical subdivision is based on the classic subdivision of the coversands by Van der Hammen (1951) and Van der Hammen and Wijmstra (1971), and the revised subdivision by Van Huissteden (1990) and Van Huissteden et al. (2001). Used abbreviations: OC = Older Coversands, YC = Younger Coversands, LLB = Lower Loamy Bed.

Meuse basin (from the Bølling onwards) and in the coversand area of the N Netherlands (during the Bølling interstadial and Early Dryas). The southernmost part of the NW European coversand belt (N Belgium and S Netherlands) remained unpopulated until the Allerød interstadial, when so-called *Federmessergruppen*, presumably originating from N France and S Germany, spread all over the NW European lowlands. The widespread occurrence of *Federmesser* settlements, which may have been a result of their highly mobile lifestyle, contrasts sharply with that of the post-*Federmesser* industries (Ahrensburgian), which tended to concentrate more strictly in regional niches, perhaps because of the rapid climatic cooling at the start of the Late Dryas stadial (Deeben & Rensink, 2005). Only from the Early Holocene (Early Mesolithic) onwards, the population density in the NW European lowlands increased again (De Bie & Vermeersch, 1998; Crombé & Cauwe, 2001).

Although the broad framework for human occupation in the NW European lowlands appears to have been established, the possible causal relationships between Late Palaeolithic to Mesolithic settlement dynamics and changes in the physical environment are poorly understood. The problems are typically related to the general lack of reliable absolute age information, which makes correlation between various proxy records difficult (De Bie & Vermeersch, 1998). Optically stimulated luminescence (OSL) dating allows determining the time of sediment deposition directly. The method uses the constituents of material that is readily available in the sedimentary context of archaeological sites, i.e. the mineral grains of the sediment itself. Several studies have demonstrated that luminescence dating is a powerful and reliable chronological tool, particularly when OSL signals from quartz are used in combination with the single-aliquot regenerative-dose (SAR) protocol (Murray & Olley, 2002; Vandenberghe et al., 2004; Koster, 2005; Wintle & Murray, 2006; Wallinga et al., 2007, and references therein; Madsen & Murray, 2009; Derese et al., 2010). So far, however, only few studies have applied the method to infer the timing of aeolian activity in Flanders (Vandenberghe et al., 2009; Buylaert et al., 2009; Derese et al., 2009; 2010). As such, the chronology of the sedimentary record in the Flemish subsurface is still poorly understood; this seriously hampers its interpretation in terms of palaeoenvironmental and -climatic changes, and makes it difficult to assess the impact of these changes on the settlement patterns in the region.

This paper reports on the application of quartz-based SAR-OSL dating to a 7 m long sediment core that was collected from a coversand ridge bordering a vast but shallow Late Glacial palaeolake, known as the Moervaart depression, in N Belgium (Fig. 2a-c). The region around the Moervaart depression including the coversand ridge (further denoted as the 'Moervaart area') is considered as a key-site for human occupation during the Late Glacial and Early Holocene, given the high amount of sites and site-complexes along the borders

https://doi.org/10.1017/S0016774600000688 Published online by Cambridge University Press

of the lake and on the coversand ridge (Crombé & Verbruggen, 2002; Sergant et al., 2009; Bats et al., 2009). Intriguingly, settlement locations seem to have changed through time and, from the Middle Holocene onwards, the area appears to have been abandoned (Bats et al., 2009). In order to understand these shifts in human occupation, it is necessary to gain insight into the evolution of the former landscape and the processes that shaped it. This forms the main subject of an interdisciplinary research project in the Moervaart area, entitled '*Prehistoric settlement and land use systems in Sandy Flanders (NW Belgium): a diachronic and geo-archaeological approach*'. The work presented here fits in with this project and specifically aims at contributing to the realisation of an absolute and robust chronological framework for the sedimentary environments in the Moervaart area.

Geological context and independent age information

The Moervaart depression is situated in the coversand area of N Belgium, in a long-stretched, largely filled palaeovalley known as the Flemish Valley (Fig. 2), which extends from the coastal plain and polder areas in the north to the hills of S Flanders in the south, and from the hills of W Flanders in the west to the cuestas of Boom and Waasland in the east (Tavernier, 1946; De Moor, 1963; Tavernier & De Moor, 1974). According to De Moor & Heyse (1978), this palaeovalley is a prominent geomorphological feature that developed during several phases of fluvial incision and infilling, as a result of the climatic fluctuations and corresponding sea level changes during the Pleistocene. The most important phase of infilling took place during the Weichselian, with the deposition of up to ~25 m fluvial and aeolian sediments in the central part of the valley. Extensive aeolian activity culminated in the accumulation of a series of west-east running coversand ridges, of which the Maldegem-Stekene coversand ridge (length: ~80 km, width: 1.5 to 3 km, height: ~5 m TAW on average; Heyse, 1979) is the most significant. This ridge is characterised by a microrelief of small ridges and irregularly shaped elongated depressions, indicating a complex depositional history.

The genesis of the Maldegem-Stekene coversand ridge, more specifically its westernmost extension near Maldegem, has been discussed in detail by Heyse (1979). The formation of the coversand ridge is thought to have started in the Late Pleniglacial, due to the climatic shift towards drier conditions and the subsequent decreasing fluvial and increasing aeolian activity in the Flemish Valley. The deflation of the Middle Pleniglacial fluvio-periglacial sands of the 'Eeklo deposit' resulted in the development of a desert pavement, locally known as the 'Middelburg Gravel'. This gravel pavement may be equivalent to the Beuningen Gravel Bed (BGB); the BGB is an important marker in the European Late Weichselian coversand stratigraphy (Fig. 1). Kolstrup (1981) constrained its formation between approximately 15,500 ^{14}C BP (~18.7 ka cal BP) and 14,000 ^{14}C BP (~17.1 ka cal BP). On the basis of SAR-OSL dating, the BGB was bracketed between 17.2±1.2 ka and 15.3±1.0 ka at Grubbenvorst (S Netherlands; Kasse et al., 2007) and between 18.2±1.3 ka and 15.9±1.1 ka at Rotem (NE Belgium; Vandenberghe et al., 2009). According to Heyse (1979), the deflated sands were resedimented as low asymmetric coversand ridges under the influence of the dominating northern winds; these aeolian sands from the lowermost part of the "Maldegem deposit" can hence be interpreted as the time-equivalent deposit of the desert pavement.

Heyse (1979) recorded the occurrence of several peat layers within the 'Maldegem deposit' around Maldegem, which were characterised mainly by *Betula* (birch) pollen and to a lesser degree by *Pinus* (pine), *Salix* (willow) and *Juniperus* (juniper). The pollenanalytic data were not interpreted in terms of age. However, radiocarbon dating of peat and wood fragments within the 'Maldegem deposit' resulted in ages between 8,825±50 ^{14}C BP (GrN-6072; 10.0-9.8 ka cal BP; 53.1% probability) and 12,010±65 ^{14}C BP (GrN-6073; 14.0-13.8 ka cal BP), i.e. Late Glacial. Consistent ages were obtained by Kolstrup & Heyse (1980) in their pollenanalytic and radiocarbon dating study on a sedimentary sequence at Langelede, situated some 5 km to the northwest of the Heidebos locality. On lithostratigraphic grounds, the profile at Langelede was interpreted as a Late Glacial sequence. This was confirmed by radiocarbon dates between 11,190±120 ^{14}C BP (GrN-8445; 13.3-13.0 cal BP) and 11,730±120 ^{14}C BP (GrN-8286; 13.8-13.5 cal BP), i.e. Allerød, for two intercalated sandy peat horizons and one moss layer. The Allerød interstadial was also recognised in the pollen stratigraphy, although it is represented at Langelede by a rather atypical pollen spectrum dominated by birch and willow. It was not possible to distinguish the Early Dryas from the Bølling, however, as the pollen diagram was found to be discontinuous and characterised by higher percentages of herbs and lower percentages of birch than the pollen spectra at other sites in the area. Kolstrup & Heyse (1980) attributed the atypical character of the record to the instability of the surface layers due to aeolian activity in the area. Although the pollen assemblage was difficult to interpret, the combined evidence did suggest that the profile at Langelede represented a more or less complete record of the Late Glacial. As such, the results of both Heyse (1979) and Kolstrup & Heyse (1980) illustrate that the development of the coversand ridges did not stop at the end of the Late Pleniglacial, but continued during the Late Glacial.

The accumulation of aeolian sand deposits blocked the drainage of the Flemish Valley to the north, which led to the development of marshy areas and peat bogs to the south of the ridge, including the Moervaart depression (De Moor & Heyse, 1978; Heyse, 1979; Spiers, 1986). This depression was filled with an alternation of aeolian sands, gyttjas or lake marls, and peat. In the past, two sequences from the deepest part of the Late

https://doi.org/10.1017/S0016774600000688 Published online by Cambridge University Press

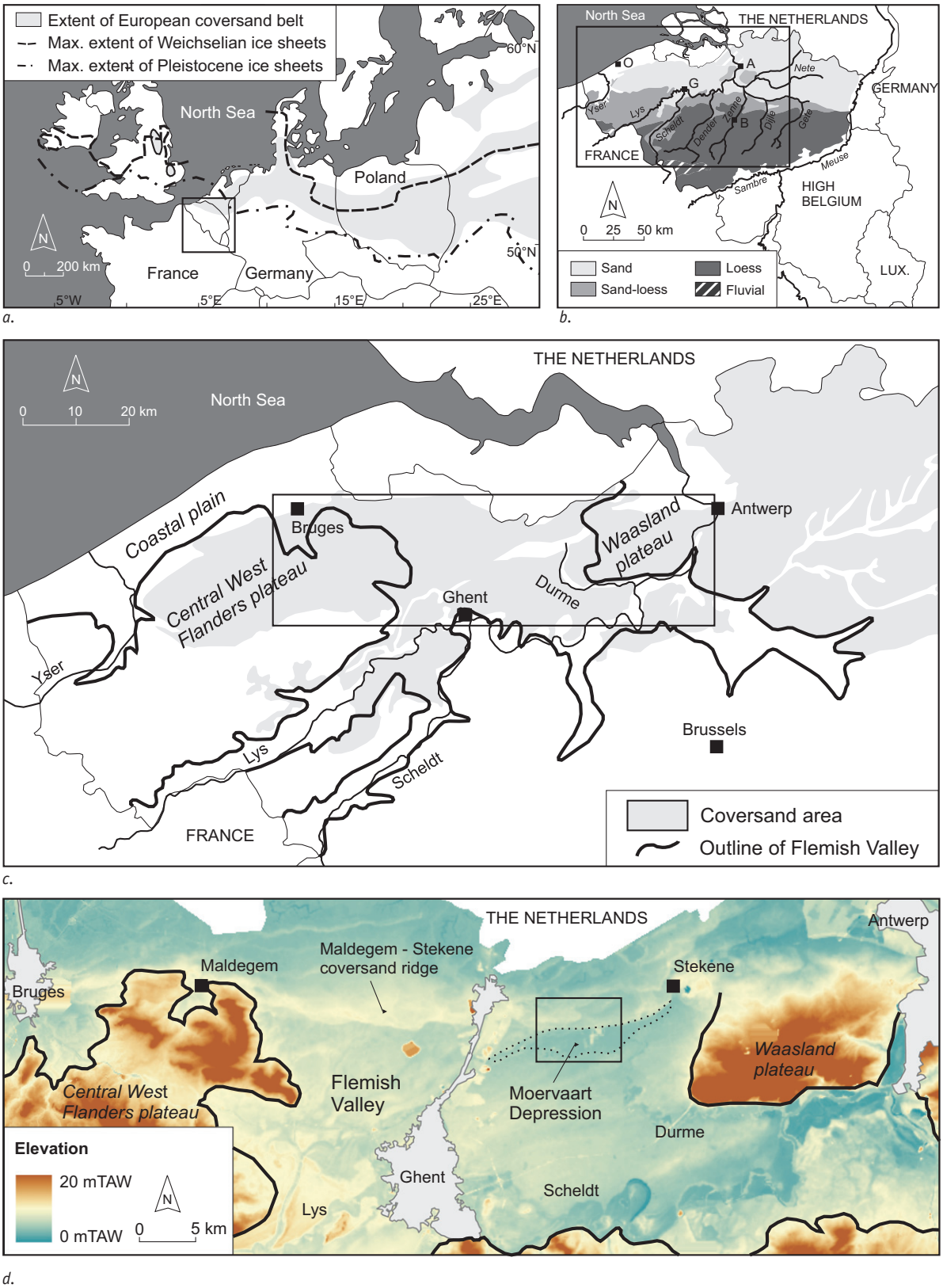

Fig. 2. a. Extent of the European coversand belt (adapted from Kasse, 1997; 2000). The location of Belgium is indicated with an open square; b. Schematic map of Belgium, showing some of the major rivers and the Pleistocene sedimentation areas in N Belgium (adapted from Paepe and Vanhoorne, 1967). The open square indicates the investigated area of the Flemish Valley; c. Extent of the coversand area and major geomorphological units in NW Belgium (adapted from Buylaert et al., 2009). The boundary of the Flemish Valley is based on Tavernier and De Moor (1974) and the coversand area on Maréchal (1992). The study area within the Flemish Valley is indicated with an open square; d. Digital elevation model of the study area, showing the main geomorphological units and the extent of the Flemish Valley (black line). The area indicated by the open square is enlarged in Fig. 3.

https://doi.org/10.1017/S0016774600000688 Published online by Cambridge University Press

Glacial lake have been studied using palynology and radiocarbon dating (Verbruggen, 1971; Van Strydonck, 2005). The ^{14}C results between 12,570±55 ^{14}C BP (KIA-18750; 15.1-14.7 ka cal BP) and 11,420±50 ^{14}C BP (KIA-18757; 13.4-13.3 ka cal BP) showed that the bulk of these sequences was deposited from the Earliest Dryas to the Allerød (Van Strydonck, 2005). The top of the sequence was placed in the Subatlantic period. This chronology has been largely confirmed by renewed multiproxy research (using e.g. pollen, spores, diatoms, chironomids, tephra, insects, mollusc) on the lake sequence (Bats et al., 2010). During the Holocene, the remaining low-lying areas, such as river valleys and depressions, were covered with flood plain sediments, while the elevated areas were locally subjected to sand-drifting (Baeté et al., 2004; Bats et al., 2009).

Stratigraphy and sedimentology of the Heidebos core

The present OSL study was carried out on a continuous (~7 m long) sedimentary sequence that was cored into the Maldegem-Stekene coversand ridge at the locality of Heidebos (X: 117031.77, Y: 207850.91 in Lambert 72 coordinates, Z: 7.293 m TAW; Fig. 3). The core locality was chosen on the ridge crest on the basis of previous exploratory studies, which reported the presence of several organic horizons within the sandy sequence. The core ('Heidebos-Wachtebeke 512') was drilled using opaque PVC tubes of 12.5 cm diameter and 1 m long. The tubes were split in half in the laboratory under subdued light conditions. One half was brought into daylight to allow a detailed description of the stratigraphy and the sediment characteristics; the other half was kept in the dark to take samples for OSL dating.

Figure 4 gives a schematic log of the sedimentary sequence. High-resolution photographs of the sequence are shown in Fig. 5. The top of the sequence consists of a podzol (0-0.5 m depth) that probably developed during the Holocene and was subsequently disturbed by intensive ploughing (to a depth of

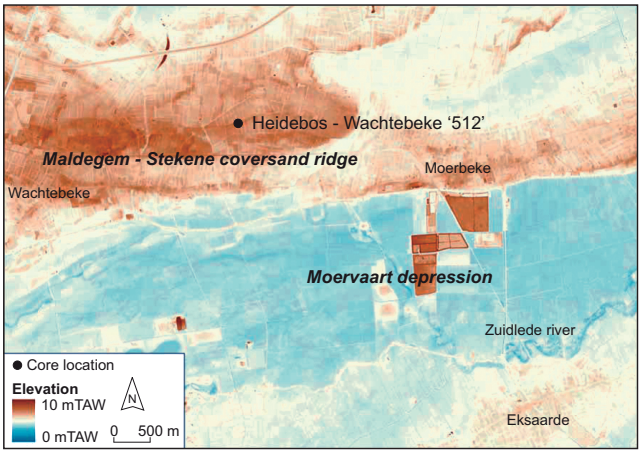

Fig. 3. Digital elevation model of the area around the Heidebos-Wachtebeke core '512', located near the top of the Maldegem-Stekene coversand ridge, to the north of the Moervaart depression.

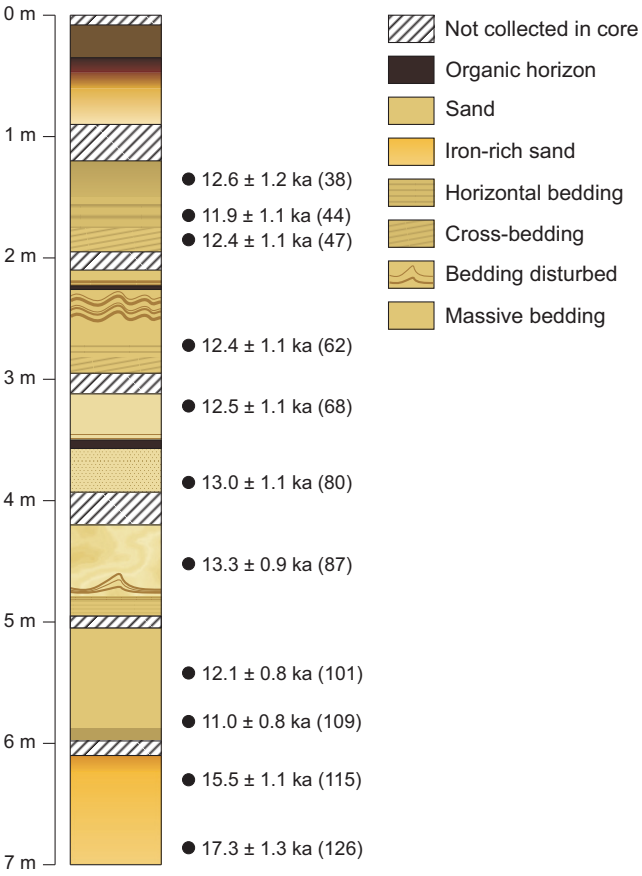

Fig. 4. Schematic log of the investigated sequence of coversands and intercalated soil horizons, showing the observed sedimentary structures and the location of the OSL samples. For each sample, the OSL age (± total uncertainty) and sample code (GLL-0907XX; XX given between brackets) are indicated on the figure.

0.4 m). The underlying unit (0.5-0.9 m) is made up of unstratified sediments that contain various amounts of organic matter and bear traces of tree rooting. In between 1 and 2 m, the sediments are composed of a ~0.3 m thick massive sand unit, followed by horizontally stratified (1.48-1.77 m) and cross-laminated (1.77-1.97 m) sands. At a depth of 2.23 m, an organic horizon of ~0.03 m thickness occurs; the immediately over- and underlying sediments show deformation structures, which are thought to originate with pressure during the drilling process. A natural origin for these deformation structures (cryoturbation) cannot be excluded, but is considered to be highly unlikely. This sequence is followed by horizontally laminated (2.71-2.80 m) and cross-bedded (2.80-2.94 m) sands. At a depth of 3.10-3.43 m, the core consists of a massive sand unit, overlying a slightly disturbed alternation of sandy and organic-rich layers. An organic horizon (3.50-3.57 m) separates this unit from a sequence of disturbed, mottled sands with a fairly high organic content. At a depth of 4.2-4.95 m, the sediments appear to be completely disturbed by the coring process, which is indicated by water-escape and deformation structures. The decalcification boundary is situated at around a depth of 5.75 m; the sediments

https://doi.org/10.1017/S0016774600000688 Published online by Cambridge University Press

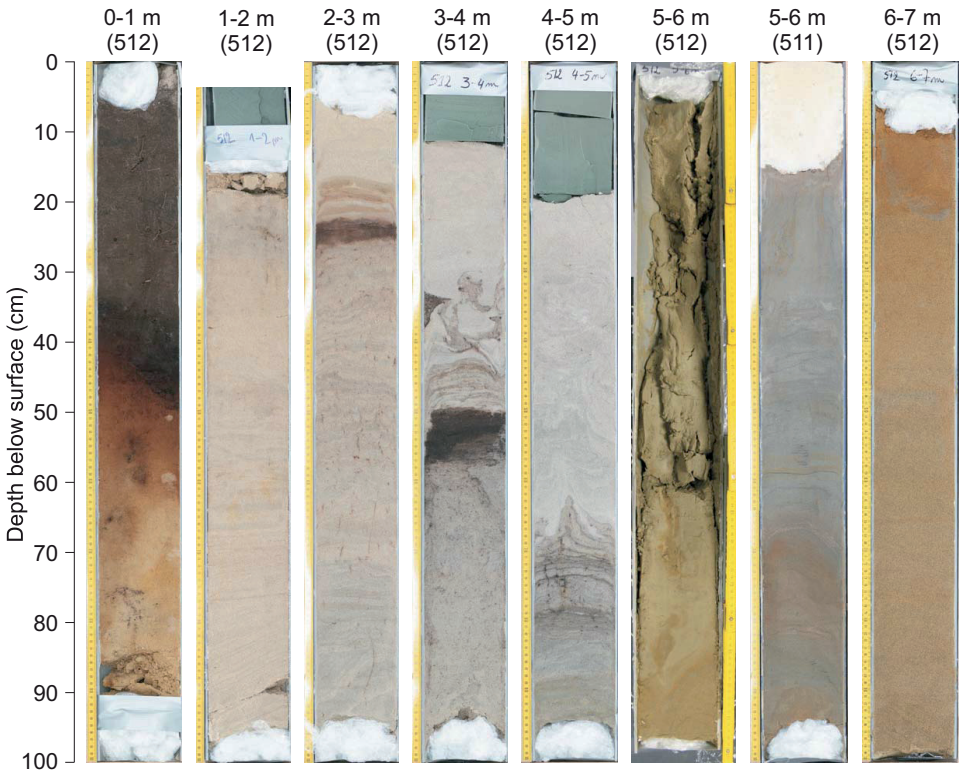

Fig. 5. High-resolution photographs of the Heidebos-Wachtebeke core '512'. The photograph of the sequence taken at a depth of 5-6 m is not a high-resolution photograph, as this half of the core was completely disturbed during the coring process and the other half was kept in the dark for OSL sampling. The equivalent part of Heidebos-Wachtebeke core '511' (taken in the vicinity of core '512') is shown to the right of the disturbed sequence.

underlying this boundary contain oxidised iron. From ~6 to 7 m, the sequence consists of massive-bedded sands with a very distinct yellow-orange colour.

Granulometric analyses on the sediments are still in progress, but qualitative observation revealed that they mainly consist of fine sands (typically 125-180 µm, or φ between +2.47 and +3). This is in agreement with the average grain sizes in the range of φ +3.47 to +1.77 (fine to very fine sands) obtained by Heyse (1979) on the sediments of the 'Maldegem deposit' in the westernmost part of the Maldegem-Stekene coversand ridge. The grain-size distribution showed that the sands are well-sorted, pointing to a transport mechanism characterised by a relatively constant energy level and transport rate. This, in combination with the sedimentary structures, led Heyse (1979) to conclude that the sands were transported and deposited by wind. The aeolian sediments are intercalated by three organic layers. So far, the nature of these organic layers is not unambiguously established. In core 'Heidebos-Wachtebeke 511' (X: 117033.25, Y: 207851.15 in Lambert 72 coordinates, Z: 7.315 m TAW), located in the vicinity of core '512', the organic layers are for the most part composed of silty sand and for 2-10% of organic matter. Therefore, none of the organic layers is thought to represent peat. In total, 100 samples were collected for pollen analysis of the sediments and intercalated organic horizons in core '511'. The analyses are still ongoing but so far, it appears that the sand samples do not or hardly contain pollen; as for the organic layers, the preliminary pollen spectra could match any period from the Late Glacial. On the whole, the sequence seems to be deposited from the Late Pleniglacial to the Holocene (Bats et al., 2010).

The range of sedimentary structures observed in the core (e.g. massive bedding, horizontal bedding, cross-lamination) illustrates the dynamic character of the sedimentary environment. The occurrence of cross-lamination may reflect the progradation of the coversand ridge. According to Heyse (1979), the Maldegem-Stekene coversand ridge advanced mainly in southern direction; our observations in the unoriented core profile do not allow confirming this. As the dune progressed, the windblown sands were increasingly transported over the windward flank of the dune, which was eroded; the erosional surface was subsequently covered with horizontally stratified sands. In the units marked by massive bedding, no macroscopically visible stratification has been observed; at present, these units are thought to be affected by syn- or post-depositional mixing processes.

Sampling, sample preparation and analytical facilities

Alternating OSL and bulk samples were collected every ~5 cm from the inner part of the sediment core (the outer 1 cm was not sampled). This resulted in 44 OSL samples and 57 bulk samples, taken for the determination of the equivalent dose and the dose rate, respectively. From these, eleven OSL samples were selected for this luminescence dating study; the selection was based on the location of these samples at the base and top of units with a distinct lithology (Fig. 4). However, the uppermost 1 m was not dated using OSL, as it might have been disturbed by post-depositional mixing (tree roots).

In the laboratory, coarse (125-180 µm) quartz grains were extracted from the OSL samples using conventional sample

https://doi.org/10.1017/S0016774600000688 Published online by Cambridge University Press

preparation techniques (treatment with HCl and H_2O_2, sieving, etching with 40% HF). The purity of the quartz extracts was confirmed by the absence of a significant infrared stimulated luminescence (IRSL) response at 60° C to a large (~50 Gy) regenerative beta dose. The sensitivity to IR stimulation was defined as significant if the resulting signal amounted to more than 10% of the corresponding OSL signal (Vandenberghe, 2004) or if the IR depletion ratio deviated more than 10% from unity (Duller, 2003).

For measurement, the quartz grains were fixed on the inner 8 mm of 9.7 mm diameter stainless steel discs using silicon spray. All OSL measurements were performed using an automated Risø TL/OSL-DA-12 reader, equipped with blue (470±30 nm) LEDs and an IR laser diode (830 nm); the quartz luminescence emissions were detected through 7.5 mm of Hoya U-340 UV filter. Details on the measurement apparatus can be found in Bøtter-Jensen et al. (2003).

Determination of the dose rate was based on high-resolution gamma-ray spectrometry. The sediment samples that were collected above and below each OSL sample were dried (at 110° C until constant weight), pulverised and homogenised. A subsample of ~140-150 g was then cast in wax (see e.g. De Corte et al., 2006) and stored for one month before being measured on top of the detector.

Luminescence characteristics

The luminescence characteristics of the quartz extracts were investigated using the SAR protocol (Murray & Wintle, 2000). Optical stimulation with the blue LEDs was for 40 s at 125° C and the initial 0.32 s of the OSL decay curve was used in all calculations, minus a background evaluated from the 1.44-2.08 s interval. Natural and regenerated signals were measured after a preheat of 10 s at 240° C, the responses to a test dose (~3.5 Gy) after a cutheat to 180° C. To minimise possible recuperation effects, a high-temperature bleach was performed after each measurement of the test dose signal by stimulating with the blue LEDs for 40 s at 280° C (Murray & Wintle, 2003). The SAR procedure involved the measurement of the natural luminescence signal, followed by the measurement of the responses to three regenerative doses (equivalent to 50%, 100% and 200% of the estimated natural dose), a zero dose and a repeat measurement of the response to the first regenerative dose. The response to the largest regenerative dose was measured twice. The second time, the sensitivity to IRSL was checked before stimulation with the blue LEDs, in order to identify aliquots with a significant feldspar contamination. The response to the zero dose was determined to evaluate whether the growth curve passes through the origin (recuperation). The measurement of the response to the lowest regenerative dose was repeated to investigate whether or not the sensitivity correction worked properly (recycling ratio). The measured aliquots were accepted if the recuperation and the IRSL/OSL ratio did not exceed a threshold set at 10% and if the recycling ratio and the IR depletion ratio did not differ more than 10% from unity. None of the aliquots had to be rejected based on these criteria.

Representative luminescence decay and growth curves are shown in Fig. 6 for one aliquot of sample GLL-090762. The OSL signal decays rapidly with stimulation time (Fig. 6, inset), which is characteristic for quartz dominated by the fast component. The dose-response curve is well approximated by a single saturating exponential function. The recycling point (open triangle on Fig. 6) matches the result of the first measurement, and the growth curve passes through the origin; this demonstrates the generally good behaviour of the samples in the SAR protocol. A dose recovery test was performed to assess the reliability of the laboratory measurement procedure (Murray & Wintle, 2003). This test was performed on three natural aliquots of each sample. The aliquots were first bleached twice for 250 s using the blue LEDs at room temperature; the two bleaching steps were separated by a 10 ks pause. Subsequently, a laboratory dose close to the expected natural dose was administered to the aliquots before any heat treatment was applied. This laboratory dose was then measured using the SAR protocol as outlined in the above. Fig. 7a summarises the dose recovery data. The recovered to given dose ratios do not differ by more than 5% from unity and, within analytical uncertainty, the given dose can be recovered to within 2.5% for all but one sample. The overall average measured to given dose ratio is 1.00±0.01 (n = 33); the corresponding overall average recycling ratio and recuperation values are 0.99±0.01 and 0.14±0.03%, respectively (Fig. 7b).

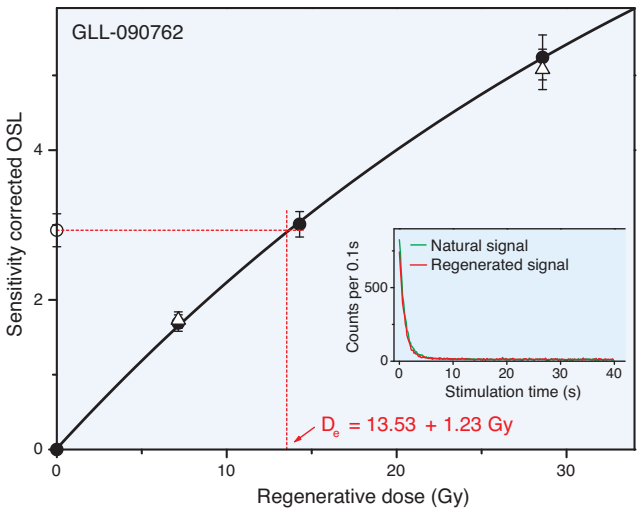

Fig. 6. Illustrative dose-response curve, and natural and regenerative OSL decay curve (inset) for an aliquot of 125-180 µm quartz grains extracted from sample GLL-090762. The solid line is the fit of the data to a single saturating exponential function. The open triangle represents a repeat measurement of the response to the first regenerative dose (recycling point). The equivalent dose (ED) is obtained by interpolation of the sensitivity-corrected natural OSL signal (open circle) on the corrected growth curve.

https://doi.org/10.1017/S0016774600000688 Published online by Cambridge University Press

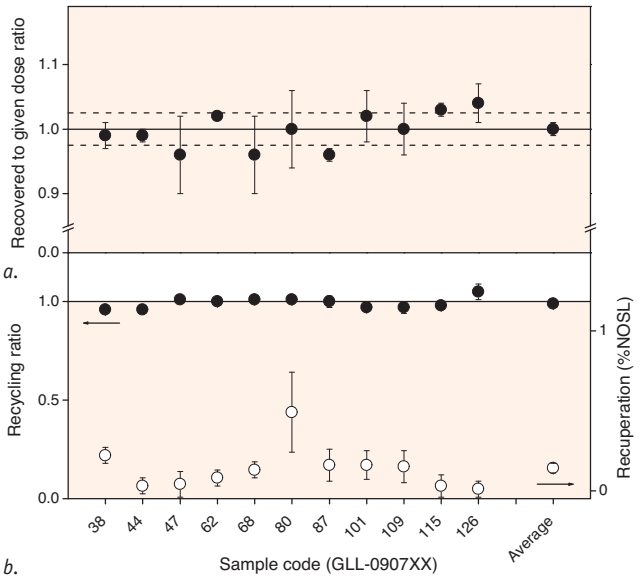

Fig. 7. Summary of the dose recovery data. a. Recovered to given dose ratios. Each datapoint represents the average (±1 standard error) of three measurements. The 'average' value represents the overall average measured to given dose ratio (±1 standard error), obtained by averaging over 33 aliquots. The solid line (eye guide) represents a recovered to given dose ratio equal to unity; the dashed lines (eye guides) bracket a 5% deviation of the ratio from unity; b. Corresponding recycling ratios (filled circles) and recuperation values (open circles). The solid line (eye guide) represents a recycling ratio equal to unity.

The results from the dose recovery tests indicate that the SAR protocol can accurately measure laboratory doses given prior to any heat treatment. For each sample, 18 replicate measurements of the equivalent dose (D_e) were made. The average values (±1 standard error) are summarised in Fig. 8a and in Table 1.

Dosimetry

The dosimetric information is summarised in Tables 1 and 2 and in Fig. 8b. The radionuclide activity concentrations obtained through high-resolution gamma-ray spectrometry were converted to dose rates using conversion factors derived from the nuclear energy releases tabulated by Adamiec & Aitken (1998). A factor of 0.9 (±5% relative uncertainty) was adopted to correct the external beta dose rates for the effects of attenuation and etching (Mejdahl, 1979). An internal dose rate in quartz grains of 0.010±0.002 Gy ka^{-1} was assumed (Vandenberghe et al., 2008). The evaluation of the time-averaged moisture content, and the corresponding correction of the dose rates, was performed following the procedure outlined in Aitken (1985). As it was not possible to take separate undisturbed samples for determination of the saturated water content, this value had to be estimated. Based on the similar lithological characteristics of the sediments and those under investigation at other coversand sites in N Belgium (Derese et al., unpublished data), the water content in fully saturated sediment (W value) was assumed to be in the range of 22% (expressed by weight); this value was used in all further calculations. Additionally, a gradient in F value (the fraction of saturation, averaged over the entire burial period) between 0.7±0.2 (at the top of the sediment sequence) and 0.9±0.1 (at the base) was adopted; the uncertainties on the F values were chosen to account for possible fluctuations in the groundwater level, which is presently situated at ~1.30 m depth. In this way, time-averaged water contents in the range of 15-20% were obtained (see Table 1). An increase in the water content of 1% increases the optical age by about 1% (or 10 years per ka). The contribution from cosmic radiation was calculated following Prescott & Hutton (1994) and a relative systematic uncertainty of 15% was associated with this value.

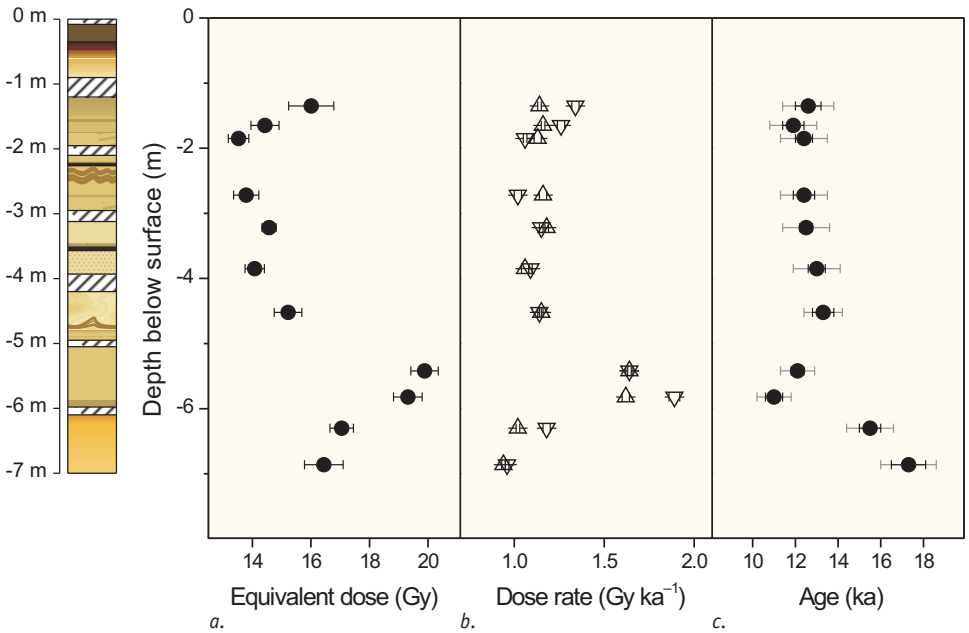

Fig. 8. Plot of the: a. equivalent doses; b. dose rates; and c. resulting optical ages as a function of the depth of the samples. The sedimentary log is the same as shown in Fig. 4. The open triangles and inverted open triangles circles represent the dose rates provided by the sediment immediately over- and underlying the OSL samples, respectively; for each sample, the average was used for calculating the OSL age. Both the random (black error bars) and total (grey error bars) uncertainties associated with the optical ages are indicated on the figure.

https://doi.org/10.1017/S0016774600000688 Published online by Cambridge University Press

Table 1. Summary of the estimated cosmic radiation, effective external dose rates provided by surrounding sediment, estimated time-averaged moisture contents, total effective dose rates (including the estimated contribution from internal radioactivity; 0.010±0.002 Gy ka^{-1}), equivalent doses (D_e), optical ages, and random (σ_r), systematic (σ_{sys}) and total (σ_{tot}) uncertainties. For each sample, the effective external dose rate was calculated as the average of the dose rate provided by the immediately over- and underlying sediment. The uncertainties mentioned with the dosimetry and D_e data are random; all uncertainties represent 1 .

Sample GLL-code	Depth (cm)	Cosmic radiation (Gy ka^{-1})	Dose rate sediment (Gy ka^{-1})	Water content (%)	Total dose rate (Gy ka^{-1})	D_e (Gy)	Age (ka)	σ_r (%)	σ_{sys} (%)	σ_{tot} (%)	(ka)
090738	133-138	0.18±0.03	1.08±0.07	15±4	1.27±0.02	16.0±0.8	12.6	5.1	7.8	9.3	1.2
090744	163-168	0.17±0.03	1.03±0.05	15±4	1.21±0.02	14.4±0.5	11.9	3.8	8.0	8.9	1.1
090747	183-188	0.17±0.03	0.92±0.04	15±4	1.10±0.02	13.5±0.4	12.4	3.2	8.0	8.6	1.1
090762	270-275	0.15±0.02	0.95±0.05	17±4	1.11±0.03	13.8±0.4	12.4	3.9	8.0	8.9	1.1
090768	320-325	0.14±0.02	1.01±0.01	17±4	1.17±0.02	14.6±0.2	12.5	2.3	8.1	8.4	1.1
090780	383-388	0.13±0.02	0.94±0.02	17±4	1.08±0.02	14.1±0.3	13.0	3.2	8.0	8.6	1.1
090787	450-455	0.12±0.02	1.009±0.003	20±2	1.14±0.02	15.2±0.5	13.3	3.5	6.2	7.1	0.9
0907101	540-545	0.11±0.02	1.519±0.002	20±2	1.64±0.02	19.9±0.5	12.1	2.8	6.3	6.8	0.8
0907109	580-585	0.11±0.02	1.6±0.1	20±2	1.75±0.04	19.3±0.5	11.0	3.3	6.2	7.1	0.8
0907115	627-632	0.10±0.02	0.99±0.08	20±2	1.10±0.02	17.0±0.4	15.5	3.1	6.2	6.9	1.1
0907126	684-689	0.10±0.01	0.84±0.01	20±2	0.95±0.02	16.4±0.7	17.3	4.5	6.2	7.7	1.3

As outlined before (section 'Coversand stratigraphy and sampling'), radionuclide activity concentrations and dose rates were obtained for the sediments over- and underlying each OSL sample. There is little variation in dose rate with depth and most values range from ~1.0 to ~1.2 Gy ka^{-1} (Fig. 8b); these values are typical for quartz-rich coversands in the NW European lowlands (see e.g. Kasse et al., 2007; Vandenberghe et al., 2009). The dose rate for samples GLL-0907101 and GLL-0907109 is somewhat higher, with values in the range of ~1.6 to 1.8 Gy ka^{-1}. The observed equilibrium in the ^{238}U series shows that precipitation of radionuclides at a later time probably does not account for the higher dose rate, as this would have resulted in a preferential enrichment of certain radioelements (e.g. radium). Moreover, the peak in dose rates was followed by a peak in equivalent dose (Fig. 8a, b). Although all samples were collected from sand layers that appeared homogeneous over a vertical distance of at least ~15 cm, and the gamma-ray spectrometric analysis was performed on ~150 g subsamples of a few 100 g of homogenised sediment, the dose rate provided by the under- and overlying sediment is not always consistent within analytical uncertainty (Table 2; Fig. 8b); the results obtained for sample GLL-0907109 illustrate this most clearly. Vandenberghe et al. (2009) previously reported that the dose rate may vary significantly in apparently homogeneous coversands. As the cause for such variations is not yet understood, the dose rate appropriate to each OSL sample was simply obtained as the mean value of the dose rate in the immediately under- and overlying sediment. The latter are given in Table 2, while the mean values are summarised in Table 1.

Luminescence ages

Table 1 synthesises all the information relevant to the age and uncertainty calculation. Uncertainties on the optical ages were calculated following the error assessment system formalised by Aitken & Alldred (1972) and Aitken (1976). It can be seen that the systematic uncertainty is dominant in the overall uncertainty on the ages and that it ranges from ~6 to 8% (Table 1).

In Fig. 8c, the resulting OSL ages, and their associated random and total uncertainties are plotted as a function of the depth of the samples. As the sources of systematic uncertainty (arising from e.g. beta source calibration, conversion of radionuclide activities to dose rates, estimation of the contribution from cosmic radiation and internal radioactivity) are largely shared between the samples, only the random uncertainty (~2-5%) is taken into account to evaluate the internal consistency of the OSL dataset. The optical ages vary between 11.0±0.4 ka and 17.3±0.8 ka. The dataset can be looked at in two different ways. When considering the whole dataset, the ages obtained for the upper 6 m of sediment (samples GLL-090738 to GLL-0907109) appear to show little increase with depth and to be spread around an average value of 12.3±0.1 ka (weighted mean ±1 expected random uncertainty); all ages are consistent with this value within 1 random uncertainty, with the exception of sample GLL-0907109 at 5.8 m depth, which is only consistent at the two sigma level. The two lowermost samples between 6 and 7 m (GLL-0907115 and -126) yield ages of 15.5±0.5 ka and 17.3±0.8 ka; within two random uncertainties, the results cannot be considered as significantly different and their weighted mean (±1 expected random uncertainty) is 16.3±0.4 ka. However, it could be argued that

https://doi.org/10.1017/S0016774600000688 Published online by Cambridge University Press

Table 2. Summary of the radionuclide activities and resulting effective dose rates (corrected for the effects of moisture and attenuation; excluding the internal radioactivity and cosmic radiation) determined for the sediment samples immediately over- and underlying the OSL samples mentioned in Table 1.

Sample GLL-code	Depth (cm)	^{40}K (Bq kg^{-1})	^{234}Th (Bq kg^{-1})	^{226}Ra (Bq kg^{-1})	^{210}Pb (Bq kg^{-1})	^{232}Th (Bq kg^{-1})	Dose rate (Gy ka^{-1})
090736	125-128	309±3	12.1±1.2	11.9±0.3	12.5±0.9	10.9±0.3	1.20±0.01
090737	128-133	298±3	7.9±0.9	10.2±0.3	9.6±0.7	9.0±0.1	1.10±0.01
090739	138-143	273±2	5.8±0.8	7.2±0.2	7.7±0.7	6.8±0.1	0.95±0.01
090743	158-163	297±4	6.1±1.0	9.4±0.3	9.7±1.1	8.7±0.2	1.08±0.01
090745	168-173	279±3	4.2±0.8	7.7±0.2	7.9±0.8	7.8±0.2	0.98±0.01
090746	178-183	264±3	3.7±0.9	6.6±0.3	5.2±0.7	6.3±0.2	0.88±0.01
090748	188-193	280±3	6.7±1.1	6.8±0.3	6.2±0.9	6.5±0.2	0.95±0.01
090761	265-270	257±2	6.4±1.2	6.4±0.3	6.0±1.1	5.6±0.1	0.86±0.01
090763	275-279	300±3	8.0±0.9	8.8±0.2	8.5±0.9	8.3±0.3	1.04±0.01
090764	281-286	277±3	7.1±0.8	7.3±0.2	8.1±1.0	6.6±0.1	0.95±0.01
090767	315-320	290±3	6.3±0.8	7.9±0.6	8.2±0.8	7.6±0.1	1.00±0.01
090769	325-330	305±3	6.4±0.9	8.7±0.3	7.3±0.8	7.7±0.2	1.03±0.01
090779	378-383	263±2	5.7±0.8	8.1±0.5	10.6±1.0	7.3±0.1	0.95±0.01
090781	388-393	256±3	5.5±1.1	7.9±0.3	10.1±1.2	7.0±0.2	0.92±0.02
090786	445-450	280±3	9.5±0.6	9.3±0.3	10.3±0.8	8.7±0.1	1.01±0.01
090788	455-460	285±3	9.2±0.7	10.0±0.6	9.5±1.0	9.1±0.2	1.01±0.01
0907100	535-540	369±4	17.2±1.6	20.0±0.7	19.8±1.1	18.3±0.2	1.52±0.02
0907102	545-550	372±3	19.5±1.3	19.6±0.3	18.5±0.8	18.1±0.3	1.52±0.01
0907108	575-580	387±4	25.1±1.8	20.6±0.5	31.2±2.3	20.6±0.2	1.77±0.03
0907110	585-590	362±3	15.3±1.5	19.9±0.8	20.2±1.4	18.3±0.2	1.50±0.02
0907114	622-627	256±3	13.7±1.2	15.4±0.4	13.2±1.2	13.3±0.2	1.06±0.02
0907116	632-637	261±3	7.0±1.0	7.9±0.2	8.5±0.7	7.6±0.2	0.91±0.01
0907125	679-684	247±3	5.4±1.2	7.1±0.2	7.8±0.7	7.4±0.1	0.86±0.01
0907127	689-694	249±3	7.0±1.0	6.7±0.3	5.8±0.8	6.6±0.2	0.83±0.01

samples GLL-0907101 and GLL-0907109, which show unexpectedly high dose rates and, in the case of sample GLL-0907109, diverging dose rates in the over- and underlying sediment (see above), should be excluded from this dataset. If done so, an increase of the age with depth may be observed within the dataset, from 12.6±0.6 ka at the top of the sequence to 17.3±0.8 ka at the base.

It is concluded that the OSL ages are generally in agreement with the stratigraphic position of the samples and form an internally consistent dataset. Although some uncertainty exists as to the uniformity of the dose rate (see above), the observed variation is not much larger than expected from individual uncertainties; this suggests that all sources of random uncertainty have been properly identified and accounted for.

Interpretation and discussion

To allow interpreting the optical ages in terms of the depositional history of the sediments and to allow a more straightforward comparison with other age information, the ages are mentioned with their total uncertainties in the following discussion. As stated in the above, the OSL dataset can be interpreted in two different ways. If all data are considered, at least two distinct phases of coversand deposition can be differentiated in the Heidebos core, one during the Late Pleniglacial (16.3±1.1 ka (n = 2) between 6-7 m depth) and one during the Late Dryas period (12.3±0.9 ka (n = 9) between 1-6 m depth). The ages thus point to a marked hiatus within the coversand sequence, which appears to encompass the early Late Glacial up to the Late Dryas. However, if the ages of 12.1±0.8 ka and 11.0±0.8 (samples GLL-0907101 and -109, respectively) are considered as unreliable and hence excluded from the dataset, the hiatus in the OSL dataset around ~6 m is much less clear and a semi-continuous coversand deposition from the final phase of the Late Pleniglacial until the Late Dryas or perhaps the Holocene (as the upper 1 m was not sampled for OSL dating) cannot be excluded. In the following, we explore the arguments pro and contra the occurrence of a marked hiatus or semi-continuous sedimentation throughout the Late Glacial.

Several sedimentary 'processes' could be held responsible for the occurrence of a gap in an OSL dataset, in this case most likely (1) non-deposition, and/or (2) erosion. A prolonged phase of land surface stability, due to the decrease or stagnation of aeolian activity, would have affected the sediment in between

https://doi.org/10.1017/S0016774600000688 Published online by Cambridge University Press

samples GLL-0907109 and GLL-0907115 by soil formation processes. We observed no such soil horizon, although it cannot be ruled out that it was present in the ~10-15 cm interval that is missing from the core; its presence may be indicated by the decalcification boundary around 5.75 m depth and by the difference in iron oxidation between the 6 m thick stack of gray-coloured sands and the lowermost 1 m thick unit of sediments with a yellow-orange colour (see Fig. 4). However, it is well documented that the Late Glacial was a period with marked climatic and environmental changes and previous investigations on equivalent coversand sequences have demonstrated that, in the NW European lowlands, aeolian coversand deposition persisted across the Late Pleniglacial to Late Glacial boundary (Vandenberghe et al., 2004; Kasse et al., 2007). At the type locality for coversand lithostratigraphy in the S Netherlands, Kasse et al. (2007) reported SAR-OSL ages between 15.3±1.0 ka and 12.7±0.9 ka for the Older Coversands II and Younger Coversands I, which represent regionally the most extensive sedimentary unit in northwest and central Europe.

As mentioned in section 'Geological context and independent age information', many Late Weichselian coversand profiles in the NW European lowlands show evidence of a large-scale deflation event at the end of the Late Pleniglacial through a lithostratigraphic horizon known as the Beuningen Gravel Bed (BGB). In the 'Heidebos-Wachtebeke 512' core, no gravel layer has been reported in the interval corresponding to the time-gap; again, it may not have been observed because this interval was incompletely sampled. In terms of time, however, it seems hard to reconcile the period of deflation that resulted in the BGB with the hiatus that may be observed in the core. Indeed, quartz-based SAR-OSL dating allowed bracketing the age of the BGB between 17.2±1.2 ka and 15.3±1.0 ka in the S Netherlands (Kasse et al., 2007) and between 18.2±1.3 ka and 15.9±1.1 ka in NE Belgium (Vandenberghe et al., 2009). It should be noted that it remains to be established whether the BGB is truly an isochronous marker. However, while it seems logical that the formation of the BGB may have started earlier at some wind-exposed localities (Kasse, 1997), it is more difficult to envisage that the conditions required to form such a widespread desert pavement (cold, dry, no or little vegetation) prevailed during the Late Glacial (warmer, wetter, increased land surface stability). The available age information thus constrains the age of the BGB to the (Late) Pleniglacial, while it would be a substantial part of the Late Glacial that is missing from the core. The hiatus could only be interpreted as a signature of local erosion, possibly caused by increased aeolian activity, at some stage between 15.5±1.1 ka and 13.3±0.9 ka.

In conclusion, it cannot be unequivocally established on the basis of the present OSL dataset whether the coversand ridge at the Heidebos locality developed during two distinct phases of aeolian deposition or whether it developed as a result of semi-continuous accumulation of aeolian sands, which was only interrupted during fairly short intervals reflected in the coversand sequence by the occurrence of disconformities (erosional surfaces between cross-laminated and horizontally laminated units). On the one hand, there is no convincing argument to exclude samples GLL-0907101 and -109 from the OSL dataset. On the other hand, the hypothesis of semi-continuous deposition is corroborated by the presence of sandy layers within the lake marl and peat sequences in the Moervaart depression (see section 'Geological context and independent age information'). As these sequences have been dated to the Late Glacial, this implies that sediment must have been available, transported and deposited during this period.

The average age of 16.3±1.1 ka (n = 2) for the lowermost 1 m of sediment matches the above-mentioned age bracket for the BGB. This could suggest that the deposition of this part of the core was coeval with the formation of this desert pavement. However, the OSL ages for the overlying 6 m of sediment also demonstrate that a significant part of the ridge at Heidebos was shaped much later. The widespread occurrence of the BGB suggests large-scale sand removal and it has been a quandary as to explain where all the deflated sand was transported to. It has been suggested that the BGB may not have (entirely) formed by deflation of the previously deposited Older Coversands I, but through accumulation of coarser material by creep or surficial runoff from higher areas, and/or that it may not be an isochronous marker (Kasse et al., 2007; see higher). An alternative explanation emerging from this and other recent optical dating studies is that the preservation potential of the original deposits of deflated sand may have been low. Indeed, optical dates for cover- and dune sands at various localities in the Netherlands and Belgium such as Ossendrecht (Vandenberghe et al., 2004), Opgrimbie (Derese et al., 2009), Arendonk and Lommel (Derese et al., unpublished data) document periods of pronounced aeolian activity throughout the Late Glacial, despite periods of rapid climate warming, wetting and land surface stability. Obviously, explaining the genesis of these deposits also requires that their source of sediment is identified.

Although the OSL dataset at present does not allow unequivocally establishing whether the coversands were deposited during two clearly separated phases of coversand deposition or not, our results allow in any case refining the ideas put forward by Heyse (1979) and Kolstrup & Heyse (1980) as to the genesis of the Maldegem-Stekene coversand ridge (see section 'Geological context and independent age information'). The luminescence chronology demonstrates that the ridge formation started during the Late Pleniglacial; moreover, it suggests that the area may have been characterised by extensive aeolian activity during the Allerød and/or Late Dryas. The OSL dataset also illustrates that the sedimentation rate increased significantly from the Late Pleniglacial (~0.5 m per ka on average) up to the Late Dryas (at least ~2 m per ka on average). It can be noted that the OSL ages do not exclude that

https://doi.org/10.1017/S0016774600000688 Published online by Cambridge University Press

one or more of the organic horizons in the Heidebos core are of Allerød age; this implies significant aeolian deposition during a phase that is generally considered as being marked by landscape stabilisation and soil formation. Interestingly, this idea does not conflict with the results obtained by Derese et al. (2009) for the dune complex at Opgrimbie (NE Belgium), where two sediment units underlying the Usselo soil of Allerød age were dated at 12.9±0.9 ka and 13.0±0.8 ka. To our view, the apparent discrepancy illustrates that the time resolution of luminescence dating techniques may be too limited to allow unambiguously correlating an aeolian unit to a particular period of the Late Glacial; on the other hand, one may wonder to what extent aeolian activity should be strictly restricted to stadials, especially as only relatively few direct sedimentation ages are available.

The OSL ages provide essential information for the landscape reconstruction in relation to the human occupation patterns during the Late Glacial - Early Holocene transition in this region. Although the optical ages and sedimentary structures do not clearly seem to point to landscape stabilisation during the Allerød, the presence of the palaeolake of the Moervaart, which by then had reached its maximal extension (Bats et al., 2010), may have favoured human settlement in the area. As a matter of fact, the first human presence did not appear earlier than the Allerød (Crombé & Verbruggen, 2002; Sergant et al., 2009; Bats et al., 2009), suggesting that the prehistoric man belonging to the *Federmesser* culture waited for favourable conditions to colonise the area. Occupation clustered mainly on the northern bank of the palaeolake and on small sandy outcrops within the lake. The extremely high density of *Federmesser* sites probably indicates a higher frequency of site re-occupation, occupation by larger groups and/or occupation for longer periods within the annual cycles compared to elsewhere in N Flanders. Clearly the massive coversand dune combined with the adjacent lake formed one of the principal 'central foci' or 'persistent places' in the Late Glacial hunter-gatherer landscape of N Flanders (Sergant et al., 2009). At some stage during the Allerød and/or Late Dryas, aeolian activity intensified dramatically, resulting in the deposition of perhaps several meters of coversands; simultaneously the palaeolake started to dry out (Bats et al., 2010). These important environmental events most likely had a considerable impact on human life. It is not unlikely that, during the Late Dryas, the environment was too inhospitable for human occupation, explaining why Final Palaeolithic societies seemingly disappeared from the area. Recolonisation took place only at the start of the Early Holocene, not before 11 ka cal BP.

Conclusions

High-resolution quartz-based SAR-OSL dating was applied to a sequence of coversands bordering the Moervaart depression at Heidebos (N Belgium). An internally consistent set of optical ages ranging from 17.3±0.8 ka to 12.6±0.6 ka was obtained, indicating sediment deposition during the Late Pleniglacial and during the Allerød and/or Late Dryas. The lowest 1 m of the sequence may be considered as the time-equivalent deposit of a desert pavement, known in the classic coversand lithostratigraphic record as the Beuningen Gravel Bed (BGB). However, the bulk of the coversand ridge at Heidebos was probably deposited during the Allerød interstadial and/or the Late Dryas stadial. It remains to be investigated to what extent the intercalated organic layers reflect phases of landscape stability; considering that uppermost 6 m of sediment may have been deposited in less than 2 ka, it is unlikely that they represent important phases of soil formation and land surface stability.

The study documents pronounced phases of aeolian activity during the Late Glacial, and contributes to an improved understanding of the environmental variables that may have influenced settlement patterns along the Moervaart area. Further investigations of the lake infill, including optical dating of clastic layers, are ongoing. It is expected that these will allow gaining further insight in the spatial and temporal relationship between the evolution of the lake and the coversand ridge, the geomorphic and climatic processes that shaped them, and how these affected the colonisation of the area.

Acknowledgements

This luminescence dating study was financially supported by the Special Research Fund of Ghent University (CD) and the Research Foundation – Flanders (FWO-Vlaanderen; DV: Postdoctoral Fellow). The technical assistance of Gilles Velghe is gratefully acknowledged. We thank K. Kasse and G. Ghysels for discussions and K. Verhoeven for his assistance with various aspects of this work. The members of the project team (M Bats, J. De Reu, Ph. De Smedt, M. Antrop, J. Bourgeois, Ph. De Maeyer, P. Finke, M. Van Meirvenne, I. Werbrouck) are gratefully acknowledged for their assistance in the field and valuable advices. The paper has been greatly improved thanks to the useful suggestions and comments of P. Kiden and J. Wallinga.

References

Adamiec, G. & Aitken, M., 1998. Dose-rate conversion factors: update. Ancient TL 16: 37-50.

Aitken, M.J., 1976. Thermoluminescence age evaluation and assessment of error limits: revised system. Archaeometry 18: 233-238.

Aitken, M.J., 1985. Thermoluminescence dating. Academic Press Inc. (London): 359 pp.

Aitken, M.J. & Alldred, J.C., 1972. The assessment of error limits in thermoluminescence dating. Archaeometry 14: 257-267.

Baeté, H., Christiaens, B., De Keersmaeker, L., Esprit, M., Van De Kerckhove, P., Vandekerkhove, K. & Walleyn, R., 2004. Bosreservaat De Heirnisse: basisrapport: situering, standplaats, historiek en onderzoek. Rapporten van het instituut voor bosbouw en wildbeheer – sectie bosbouw 18. Instituut voor Bosbouw en Wildbeheer (Geraardsbergen): 108 pp.

Bats, M., De Reu, J., De Smedt, P., Antrop, M., Bourgeois, J., Court-Picon, M., De Meyer, P., Finke, P., Van Meirvenne, M., Verniers, J., Werbrouck, I., Zwertvaegher, A. & Crombé, P., 2009. Geoarchaeological research of the large palaeolake of the Moervaart (municipalities of Wachtebeke and Moerbeke-Maas, East Flanders, Belgium). From Late Glacial to Early Holocene. Notae Praehistoricae 29: 105-112.

Bats, M., De Reu, J., De Smedt, P., Antrop, M., Bourgeois, J., Court-Picon, M., De Meyer, P., Finke, P., Van Meirvenne, M., Verniers, J., Werbrouck, I., Zwertvaegher, A. & Crombé, P., 2010. Continued geoarchaeological research of the large palaeolake of the Moervaart: a preliminary report of the 2010 campaign. Notae Praehistoricae 30: 15-21.

Bos, J.A.A. & Janssen, C.R., 1996. Local impact of Palaeolithic man on the environment during the end of the Last Glacial in the Netherlands. Journal of Archaeological Science 23: 731-739.

Bronk Ramsey, C., 2009. Bayesian analysis of radiocarbon dates. Radiocarbon 51: 337-360.

Buylaert, J.-P., Ghysels, G., Murray, A.S., Thomsen, K.J., Vandenberghe, D., De Corte, F., Heyse, I. & Van den haute, P., 2009. Optical dating of relict sand wedges and composite-wedge pseudomorphs in Flanders, Belgium. Boreas 38: 160-175.

Bøtter-Jensen, L., Andersen, C.E., Duller, G.A.T. & Murray, A.S., 2003. Developments in radiation, stimulation and observation facilities in luminescence measurements. Radiation Measurements 37: 535-541.

Crombé, Ph. & Cauwe, N., 2001. The Mesolithic. *In:* Cauwe, N., Hauzeur, A. & van Berg, P.-L. (eds): Prehistory of Belgium. Special issue on the occasion of the XIVth Congress of the International Union for Prehistoric and Protohistoric Sciences. Bulletin de la Société royale belge d'Anthropologie et de Préhistoire 112: 49-62.

Crombé, Ph. & Verbruggen, C., 2002. The Lateglacial and early Postglacial occupation of northern Belgium: the evidence from Sandy Flanders. *In:* Eriksen, B.V. & Bratlund, B. (eds): Recent studies in the Final Palaeolithic of the European plain. Proceedings of a UISPP Symposium, Stockholm 1999. Jutland Archaeological Society Publications: 165-180.

De Bie, M. & Vermeersch, P.M., 1998. Pleistocene-Holocene transition in Benelux. Quaternary International 49/50: 29-43.

De Corte, F., Vandenberghe, D., De Wispelaere, A., Buylaert, J.-P. & Van den haute, P., 2006. Radon loss from encapsulated sediments in Ge gamma-ray spectrometry for the annual radiation dose determination in luminescence dating. Czech Journal of Physics 56: D183-D194.

Deeben, J. & Rensink, E., 2005. Het Laat-Paleolithicum in Zuid-Nederland. *In:* Deeben, J., Drenth, E., van Oorsouw, M.-F. & Verhart, L. (eds): De Steentijd van Nederland. Archeologie 11/12: 171-199.

De Moor, G., 1963. Bijdrage tot de kennis van de fysische landschapsvorming in Binnen-Vlaanderen. Tijdschrift van de Belgische Vereniging voor Aardrijkskundige Studies 32: 329-433.

De Moor, G. & Heyse, I., 1978. De morfologische evolutie van de Vlaamse Vallei. De Aardrijkskunde 4: 343-375.

Derese, C., Vandenberghe, D., Paulissen, E. & Van den haute, P., 2009. Revisiting a type locality for Late Glacial aeolian sand deposition in NW Europe: Optical dating of the dune complex at Opgrimbie (NE Belgium). Geomorphology 109: 27-35.

Derese, C., Vandenberghe, D., Eggermont, N., Bastiaens, J., Annaert, R. & Van den haute, P., 2010. A medieval settlement caught in the sand: Optical dating of sand-drifting at Pulle (N Belgium). Quaternary Geochronology 5: 336-341.

Duller, G.A.T., 2003. Distinguishing quartz and feldspar in single grain luminescence measurements. Radiation Measurements 37: 161-165.

Heyse, I., 1979. Bijdrage tot de geomorfologische kennis van het noordwesten van Oost-Vlaanderen (België). Verhandelingen van de Koninklijke Academie voor Wetenschappen, Letteren en Schone Kunsten van België 40: 217 pp.

Hoek, W.Z., 2001. Vegetation response to the ~14.7 and ~11.5 ka cal BP climate transitions: is vegetation lagging climate? Global and Planetary Change 30: 103-115.

Kasse, C., 1997. Cold-climate aeolian sand-sheet formation in North-Western Europe (c. 14-12.4 ka); a response to permafrost degradation and increased aridity. Permafrost and Periglacial Processes 8: 295-311.

Kasse, C., 2002. Sandy aeolian deposits and environments and their relation to climate during the Last Glacial Maximum and Lateglacial in northwest and central Europe. Progress in Physical Geography 26: 507-532.

Kasse, C., Vandenberghe, D., De Corte, F. & Van den haute, P., 2007. Late Weichselian fluvio-aeolian sands and coversand of the type locality Grubbenvorst (southern Netherlands): sedimentary environments, climate record and age. Journal of Quaternary Science 22: 695-708.

Kolstrup, E., 1980. Climate and stratigraphy in northwestern Europe between 30,000 BP and 13,000 BP, with special reference to the Netherlands. Mededelingen Rijks Geologische Dienst 32: 181-253.

Kolstrup, E. & Heyse, I., 1980. A different Late-Glacial vegetation and its environment in Flanders (Belgium). Pollen et Spores 22: 469-481.

Koster, E.A., 2005. Recent advances in luminescence dating of Late Pleistocene (cold-climate) aeolian sand and loess deposits in Western Europe. Permafrost and Periglacial Processes 16: 131-143.

Madsen, A.T. & Murray, A.S., 2009. Optically stimulated luminescence dating of young sediments: A review. Geomorphology 109: 3-16.

Maréchal, R., 1992. Géologie du Quaternaire, lithologie des terrains superficiels. Deuxième Atlas de Belgique. National Institute of Geography, Commission of the National Atlas (Brussels): 25 pp.

Mejdahl, V., 1979. Thermoluminescence dating: beta-dose attenuation in quartz grains. Archaeometry 21: 61-72.

Murray, A.S. & Olley, J.M., 2002. Precision and accuracy in the optically stimulated luminescence dating of sedimentary quartz: a status review. Geochronometria 21: 1-16.

Murray, A.S. & Wintle, A.G., 2000. Luminescence dating of quartz using an improved single-aliquot regenerative-dose protocol. Radiation Measurements 32: 57-73.

Murray, A.S. & Wintle, A.G., 2003. The single aliquot regenerative dose protocol: potential for improvements in reliability. Radiation Measurements 37: 377-381.

Paepe, R. & Vanhoorne, R., 1967. The stratigraphy and palaeobotany of the Late Pleistocene in Belgium. Toelichtende Verhandelingen voor de Geologische Kaart en Mijnkaart van België 8: 96 pp.

https://doi.org/10.1017/S0016774600000688 Published online by Cambridge University Press

Prescott, J.R. & Hutton, J.T., 1994. Cosmic ray contributions to dose rates for luminescence and ESR dating: large depths and long-term time variations. Radiation Measurements 23: 497-500.

Reimer, P.J., Baillie, M.G.L., Bard, E., Bayliss, A., Beck, J.W., Blackwell, P.G., Bronk Ramsey, C., Buck, C.E., Burr, G.S., Edwards, R.L., Friedrich, M., Grootes, P.M., Guilderson, T.P., Hajdas, I., Heaton, T.J., Hogg, A.G., Hughen, K.A., Kaiser, K.F., Kromer, B., McCormac, F.G., Manning, S.W., Reimer, R.W., Richards, D.A., Southon, J.R., Talamo, S., Turney, C.S.M., Van der Plicht, J. & Weyhenmeyer, C.E., 2009. IntCal09 and Marine09 radiocarbon age calibration curves, 0-50,000 years cal BP. Radiocarbon 51: 1111-1150.

Renssen, H., Kasse, C., Vandenberghe, J. & Lorenz, S.J., 2007. Weichselian Late Pleniglacial surface winds over northwest and central Europe: a model-data comparison. Journal of Quaternary Science 22: 281-293.

Sergant, J., Crombé, Ph. & Perdaen, Y., 2009. Mesolithic territories and land-use systems in north-western Belgium. *In:* McCartan, S.B., Schulting, R., Warren, G. & Woodman, P. (eds): Mesolithic Horizons. Papers presented at the Seventh International Conference on the Mesolithic in Europe, Belfast 2005, Oxbow Books (Oxford): 277-281.

Spiers, V., 1986. Mineralogisch en petrografisch onderzoek van de kalkrijke sedimenten van de Moervaartdepressie. Licentiaatsverhandeling, Rijksuniversiteit Gent (Gent): 61 pp.

Street, M., 1998. The archaeology of the Pleistocene-Holocene transition in the northern Rhineland, Germany. Quaternary International 49/50: 45-67.

Tavernier, R., 1946. L'évolution du Bas Escaut au Pleistocène supérieur. Bulletin de la Société belge de Géologie, Paléontologie et Hydrologie 55: 106-125.

Tavernier, R. & De Moor, G., 1974. L'évolution du basin de l'Escaut. *In:* Macar, P. (ed.): L'évolution quaternaire des bassins fluviaux de la Mer du Nord méridionale. Colloque du Centenaire de la Société Géologique de Belgique, Liège: 159-233.

Terberger, Th., Barton, N. & Street, M., 2009. The Late Glacial reconsidered - recent progress and interpretations. *In:* Street, M., Barton, N. & Terberger, Th. (eds): Humans, environment and chronology of the late glacial of the North European Plain. Proceedings of Workshop 14 of the 15th UISPP Congress, Lisbon, September 2006. RGZM Tagungen, 6: 189-207.

Vandenberghe, D., 2004. Investigation of the optically stimulated luminescence dating method for application to young geological samples. Ph.D. thesis, Universiteit Gent (Gent): 358 pp.

Vandenberghe, D., De Corte, F., Buylaert, J.-P., Kučera, J. & Van den haute, P., 2008. On the internal radioactivity in quartz. Radiation Measurements 43: 771-775.

Vandenberghe, D., Kasse, C., Hossain, S.M., De Corte, F., Van den haute, P., Fuchs, M. & Murray, A.S., 2004. Exploring the method of optical dating and comparison of optical and ^{14}C ages of Late Weichselian coversands in the southern Netherlands. Journal of Quaternary Science 19: 73-86.

Vandenberghe, D., Vanneste, K., Verbeeck, K., Paulissen, E., Buylaert, J.-P., De Corte, F. & Van den haute, P., 2009. Late Weichselian and Holocene earthquake events along the Geleen fault in NE Belgium: OSL age constraints. Quaternary International 199: 56-74.

Van der Hammen, T., 1951. Late glacial flora and periglacial phenomena in the Netherlands. Leidse Geologische Mededelingen 17: 71-183.

Van der Hammen, T., Wijmstra, T.A., 1971. The Upper Quaternary of the Dinkel valley (Twente, Eastern Overijssel, the Netherlands). Mededelingen Rijks Geologische Dienst 22: 55-212.

Van Huissteden, J., 1990. Tundra rivers of the last glacial: sedimentation and geomorphological processes during the Middle Pleniglacial in Twenten eastern Netherlands. Mededelingen Rijks Geologische Dienst 44: 3-138.

Van Huissteden, J., Schwan, J.C.G. & Bateman, M.D., 2001. Environmental conditions and paleowind directions at the end of the Weichselian Late Pleniglacial recorded in aeolian sediments and geomorphology (Twente, Eastern Netherlands). Geologie en Mijnbouw / Netherlands Journal of Geosciences 80: 1-18.

Van Strydonck, M., 2005. Radiocarbon dating. *In:* Crombé (ed.): The last hunter-gatherer-fisherman in Sandy Flanders (NW Belgium). The Verrebroek and Doel excavation projects (Vol. 1). Archaeological Reports Ghent University (Gent): 127-130.

Verbruggen, C., 1971. Postglaciale landschapsgeschiedenis van zandig Vlaanderen. Botanische, ecologische en morfologische aspekten op basis van palynologisch onderzoek. Ph.D. thesis, Rijksuniversiteit Gent (Gent): 440 pp.

Wallinga, J., Davids, F. & Dijkmans, J.W.A., 2007. Luminescence dating of Netherlands' sediments. Netherlands Journal of Geosciences / Geologie en Mijnbouw 86: 179-196.

Wintle, A.G. & Murray, A.S., 2006. A review of quartz optically stimulated luminescence characteristics and their relevance in single-aliquot regeneration dating protocols. Radiation Measurements 41: 369-391.

https://doi.org/10.1017/S0016774600000688 Published online by Cambridge University Press